How thermodynamic environments control stratocumulus microphysics and interactions with aerosols

Environmental Research Letters

LETTER

How thermodynamic environments control stratocumulus microphysics and interactions with aerosols

Hendrik Andersen and Jan Cermak

Department of Geography, Ruhr-Universität Bochum, Universitätsstraße 150, D-44780 Bochum, Germany

E-mail: hendrik.andersen@rub.de

Keywords: stratocumulus microphysics, aerosol–cloud interactions, thermodynamic environments, saturation effects, MODIS, ERA-Interim

Supplementary material for this article is available online

OPEN ACCESS

RECEIVED
2 October 2014

REVISED
12 January 2015

ACCEPTED FOR PUBLICATION
16 January 2015

PUBLISHED
29 January 2015

Abstract

Aerosol–cloud interactions are central to climate system changes and depend on meteorological conditions. This study identifies distinct thermodynamic regimes and proposes a conceptual framework for interpreting aerosol effects. In the analysis, ten years (2003–2012) of daily satellite-derived aerosol and cloud products are combined with reanalysis data to identify factors controlling Southeast Atlantic stratocumulus microphysics. Considering the seasonal influence of aerosol input from biomass burning, thermodynamic environments that feature contrasting microphysical cloud properties and aerosol–cloud relations are classified. While aerosol impact is stronger in unstable environments, it is mostly confined to situations with low aerosol loading (aerosol index AI $\lesssim 0.15$), implying a saturation of aerosol effects. Situations with high aerosol loading are associated with weaker, seasonally contrasting aerosol-droplet size relationships, likely caused by thermodynamically induced processes and aerosol swelling.

1. Motivation and aim

Atmospheric aerosols can alter cloud properties by acting as cloud condensation nuclei, facilitating the formation of cloud droplets. Assuming a constant cloud water content, a higher concentration of droplets leads to smaller droplet radii, a larger overall droplet surface area and thus an increase in cloud albedo (Twomey 1977). Cloud lifetime (Albrecht 1989) and cloud vertical extent (Pincus and Baker 1994) are also thought to be modified by concomitant changes in precipitation susceptibility. However, the level of scientific understanding concerning aerosol–cloud interactions (ACI) is low (Boucher *et al* 2013), as these processes are linked to many factors like cloud regime (Stevens and Feingold 2009) or meteorology (e.g. Loeb and Schuster 2008, Su *et al* 2010), leading to a high process complexity.

This study focuses on the impact of aerosols on stratocumulus microphysics in the Southeast Atlantic. Stratocumulus clouds play an important role in the Earth's climate system not only because of their great spatial abundance, but also because their shortwave cloud albedo radiative effect is greater than their longwave radiative effect, resulting in a net negative radiative effect (Hartmann *et al* 1992). As the Earth's radiative budget is sensitive to the modification of stratiform clouds (Randall *et al* 1984), elucidating their interactions with aerosols is of particular interest. Past studies (e.g. Klein and Hartmann 1993, Matsui *et al* 2004, 2006, Chen *et al* 2014, Koshiro and Shiotani 2014) have shown that microphysical characteristics of clouds, as well as the overall stratocumulus amount are governed in part by lower-tropospheric stability (LTS). Matsui *et al* (2004) found that aerosol impact on cloud droplet radius is stronger in more dynamic environments that feature a lower LTS and argue that very high LTS environments dynamically suppress cloud droplet growth and reduce ACI intensity. In any of these environments, the loading of atmospheric aerosols is an important factor, as Bréon *et al* (2002) showed that on a global scale, aerosol impact on cloud droplet size is saturated with high aerosol loadings (aerosol index AI $\gtrsim 0.15$). In the Southeast Atlantic, aerosol loading is largely controlled by the biomass burning season (BBS) in Africa (Kaufman *et al* 2005a). The burning of biomass reaches a maximum intensity from July to September,

with trade winds transporting a large portion of these aerosols over the Atlantic Ocean (Anderson *et al* 1996, Edwards *et al* 2006). However, these aerosols are often transported above and well separated from the cloud deck, physically limiting interactions between aerosols and clouds (Keil and Haywood 2003, Labonne *et al* 2007, Costantino and Bréon 2013, Painemal *et al* 2014) while increasing uncertainty in the retrieval of cloud properties (Meyer *et al* 2013). Further complicating analyses, aerosols and cloud properties tend to covary with similar meteorological variables (e.g. - relative humidity (RH)). This covariation is caused by aerosol swelling in humid environments (e.g. Haywood *et al* 1997, Charlson *et al* 2007, Myhre *et al* 2007, Jones *et al* 2009).

The goal of this study is to analyze aerosol impact on cloud microphysics in the stratocumulus regime, laying a specific focus on the influence of the suspected key factors LTS, RH and aerosol loading. The novelty of this study's approach is the combined analysis of ACI sensitivity to aerosol loading (Bréon *et al* 2002) and LTS (Matsui *et al* 2004) in a regime based approach as suggested by Stevens and Feingold (2009), enabling a profound view into the aerosol-stratocumulus-meteorology system.

The guiding hypothesis of this study is:

The magnitude of aerosol impact on stratocumulus microphysics is largely controlled by the atmospheric aerosol loading and thermodynamically induced processes.

2. Data and methods

2.1. Data sets and preprocessing

Two different data sets are used in this study. Aerosol and cloud data are based on daily level 3 collection 5.1 (L3 C5.1) products of Terra's Moderate Resolution Imaging Spectroradiometer (MODIS) sensor (Platnick *et al* 2003, Levy *et al* 2009). For information on the atmospheric aerosol loading, the AI, the product of aerosol optical depth (AOD, 0.55 μm; data set: Optical_Depth_Land_And_Ocean_Mean) and Ångström exponent (0.55 and 0.865 μm; data set: Angstrom_Exponent_1_Ocean_Mean), is used (Costantino and Bréon 2013). AI has been identified as a better proxy for aerosol number concentration than AOD, weighting the fine mode stronger than AOD alone (Nakajima *et al* 2001). Stratocumulus microphysics are frequently represented by cloud droplet number concentration (e.g. Quaas *et al* 2006). Here, MODIS cloud-top droplet effective radius (CDR; data set: Cloud_Effective_Radius_Liquid_Mean) is used, as the retrieval of cloud droplet number concentration requires additional assumptions, leading to increased uncertainty (Brenguier *et al* 2000).

As a quality filter on the MODIS data, L3 retrievals that are based on level 2 pixels with a standard deviation exceeding the mean are eliminated. To reduce measurement artefacts due to cloud contamination of aerosol retrievals (Grandey *et al* 2013), scenes with cloud fraction (CLF) >0.93 were excluded from the analysis. L3 retrievals with a mean cloud-top temperature <273 K are filtered out with the intention to ensure that only liquid clouds are considered (assuming no overlying thin clouds). For statistical analyses, AI and CDR data are log-transformed and linearly detrended, subtracting the mean of each data point, so that the mean equals zero (Wilson *et al* 2001, Stier *et al* 2005). In order to avoid computation errors during the logarithmic transformation as consequence of occurrences of the value '0' (log(0) is not defined), data is manipulated by adding a minuscule quantity (10^{-6}) to each data point (for information on data distributions see supplementary material available online at stacks.iop.org/erl/10/024004/mmedia).

ERA-Interim data is applied in this study to provide large-scale information on RH and LTS. ERA-Interim is the most recent generation of reanalysis data produced by the European Centre for Medium-Range Weather Forecasts (ECMWF). It covers the period from 1979 onwards and continues to be extended forward in near real time (Dee *et al* 2011). The applied products are available in horizontal resolutions of $0.75° \times 0.75°$ at 37 pressure levels in time-steps of 6 hours (www.ecmwf.int/research/era/do/get/era-interim. The 12:00 UTC time step is used as it is closest to the daytime Terra observations in the study area (approximately between 9:30 and 10:30 am UTC (Hubanks *et al* 2008)). LTS is not a readily available reanalysis product but can be computed as

$$\Delta\theta = \theta(p = 700\ \text{hPa}) - \theta(p = \text{SLP}). \quad (1)$$

(Klein and Hartmann 1993), where $\Delta\theta$ is the difference in potential temperature between 700 hPa and the surface. It can be interpreted as a measure for inversion strength or static stability of the lower troposphere (Klein and Hartmann 1993). RH data are used from the pressure level at 950 hPa, as ERA-Interim CLF is greatest at this level. At an original spatial resolution of $0.75° \times 0.75°$, LTS and RH data are linearly interpolated to fit the $1° \times 1°$ MODIS grid. While this relatively coarse spatial resolution impairs the analysis of RH effects (sub-grid variability of humidity impacts aerosol retrievals (Haywood *et al* 1997)), large-scale humidity may still help to uncover tendencies of aerosol swelling.

2.2. Methods

As stratocumulus clouds are the dominant cloud type in the Southeast Atlantic (Klein and Hartmann 1993), a more homogeneous time series of cloud properties implies a stronger stratocumulus prevalence. The coefficient of variation (standard deviation divided by mean) of CDR, CLF, cloud-top temperature, cloud liquid water path (LWP) and cloud optical depth was used to estimate this cloud homogeneity in $1° \times 1°$ grid cells in the Southeast Atlantic. On this basis, the study

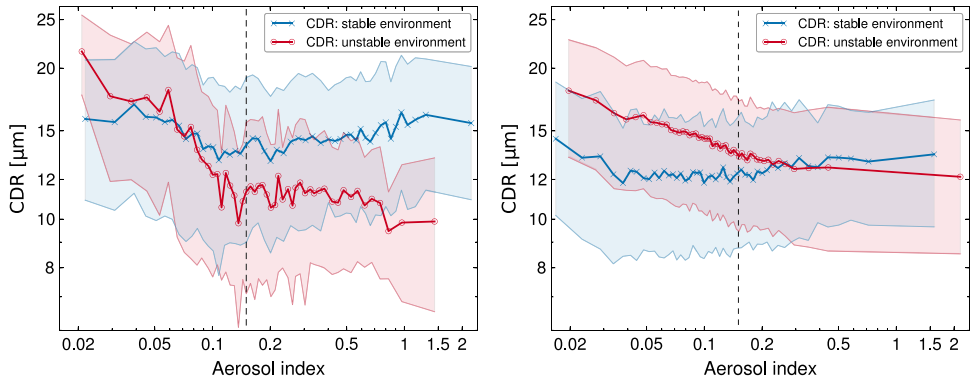

Figure 1. Mean cloud-top droplet effective radius (log-scaled) as a function of equal-size bins of AI (log-scaled) in different thermodynamic environments for the biomass burning season (left) and the other months (right). Shaded areas represent the interquartile range. The stable environment is colored in blue, the unstable environment is colored in red. The dashed vertical line represents the saturation point as identified by (Bréon *et al* 2002).

area (10°S–20° S and 0° E–11° E) was delineated qualitatively. It is in good agreement with the stratocumulus region used by Klein and Hartmann (1993), but extends 1° further to the east.

To investigate the roles of aerosol loading and LTS on interactions between aerosols and cloud microphysics, the data sets are divided into two time periods (July–September (BBS); other months (OM)) to acknowledge the vastly different vertical structure and chemical properties of aerosol plumes during the BBS. Data is additionally split up into different environments by discriminating.

(1) Two LTS environments

   (a) unstable environment: <25th percentile of LTS data

   (b) stable environment: >75th percentile of LTS data(the 2nd and 3rd quartiles are excluded for more clearly separated environments and reduced intra-group LTS variability).

(2) Two aerosol environments based on the saturation mechanism identified by Bréon *et al* (2002):

   (a) low aerosol loading environment: AI $\leqslant$ 0.15

   (b) high aerosol loading environment: AI > 0.15.

Data analysis is performed by binning the previously subdivided data of these environments into equally sized bins, each bin containing one percent of the considered data points.

3. Results and discussion

Figure 1 shows mean and interquartile range (IQR) of CDR in equally sized AI bins during the BBS (left panel) and the OM (right panel), for the two thermodynamic environments described above. Each environment features 50 bins. The unstable regime in BBS features ≈500 data points, all other regimes contain at least 10000 data points. During both time periods, mean droplet sizes in the unstable environment are larger than in the stable environment (red color) at low aerosol loadings (AI smaller than 0.15), and smaller with high aerosol loadings, resulting in a steeper overall slope. This suggests a stronger aerosol impact on CDR in this environment, especially during the BBS. In accordance with findings by Bréon *et al* (2002) a clear saturation of aerosol impact with high aerosol loading is apparent in the unstable environments. Cloud droplet response to changes in aerosol loading is different in the stable environments, as mean droplet sizes are not similarly sensitive to changes in AI (slope is small in unstable environments). During the BBS, mean CDR even increases slightly with high AI. While some of this weaker CDR sensitivity to aerosols may be caused by more frequently separated aerosol and cloud layers or a reduced susceptibility due to smaller droplets, this does not explain the tendency of increasing droplet sizes with high aerosol loadings during the BBS. In these situations, mean bin LWP (not shown) is substantially higher, possibly due to reduced dry air entrainment (Johnson *et al* 2004). Thus it seems likely that the observed absolute differences in CDR between stable and unstable environments are driven by cloud dynamical effects (CDR and LWP are positively associated (Painemal *et al* 2014)) or ambient meteorology. It is unlikely that the observed CDR–AI relationships can be ascribed to CLF based artefacts, as bin mean CLF (not shown) does not show similar patterns. Generally, a clear separation of the two stability environments based on droplet sizes is not possible as the internal variability is relatively high, leading to a large overlap of the data points within the IQR (shaded areas). Still, the behavior found in both environments differs markedly, even when considering the wide IQR margins.

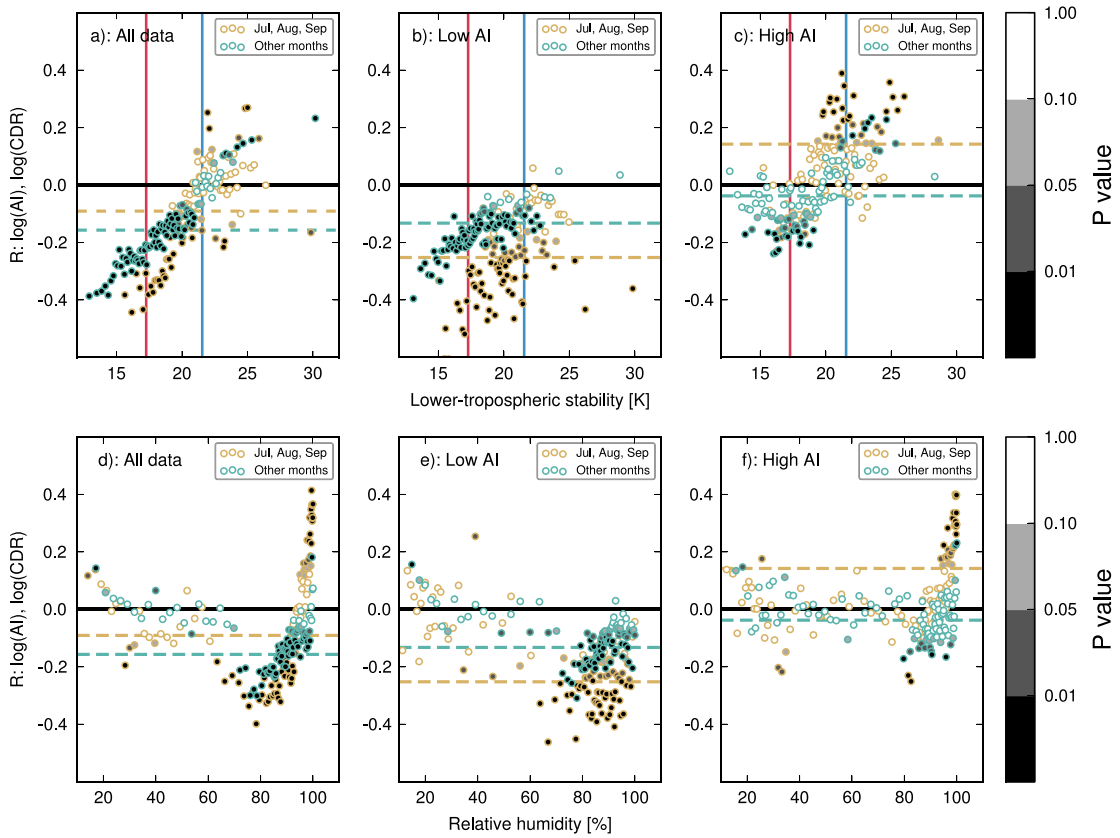

Figure 2. Bin-correlations of log(AI) and log(CDR) as a function of LTS in the top row (limits of stability environments are indicated by vertical lines) and as a function of RH in the bottom row for the two time periods. The entire data sets are shown in the left-hand column (a), low (AI < 0.15) and high aerosol loading environments (AI > 0.15) respectively are illustrated in the center (b) and right-hand (c) columns. The dashed lines represent Pearson *r* for all seasonal data contained in each sub-figure. The shade of gray in the center of each dot illustrates the probability value of the correlation (level of significance).

Figure 2 illustrates log(AI)–log(CDR) correlations in bins of LTS percentiles (top row) and RH percentiles (bottom row) for both time periods. The bins contain between 110 (BBS) and 700 (OM) data points for the subdivided data sets and between 1000 (BBS) and 3000 (OM) data points when considering the entire data sets. The position and orientation of the scatter gives information about the tendency of ACI occurrences (position on the *y*-axis) and the magnitude of the impact of the meteorological parameter (orientation/slope of the point cloud). While figures in the left-hand column are based on the entire data sets of each time period, data is subdivided into low aerosol environments (AI < 0.15) in the center column and high aerosol environments (AI > 0.15) in the right-hand column. It is apparent that the statistical relationship between log(AI) and log(CDR) is dependent on both LTS and RH and that this dependency is connected to the property of the given meteorological parameter and the aerosol environment.

Considering the entire data sets, log(AI) and log (CDR) are weakly associated (r : −0.09 in BBS, −0.16 in OM). However, this association is heavily dependent on LTS in both time periods, as stable and unstable environments feature contrasting log(AI)–log(CDR) relationships that can be clearly separated in both time periods. While the unstable environment exclusively features negative associations, log(AI) and log(CDR) are mostly positively associated in the stable environment. In low aerosol environments (figure 2(b)), a stronger overall correlation can be identified, especially in the BBS (r : −0.25 in BBS, −0.13 in OM). The stronger correlations in the BBS may be explained by the high potential of biomass burning aerosols (mostly black and organic carbon) to act as CCN (Andreae and Rosenfeld 2008). The strong effect of LTS on the log(AI)–log(CDR) relationship is mitigated to some extent, as log(AI) and log(CDR) associations are mostly negative, indicating that in these situations, aerosols may be the main factor impacting cloud microphysics, showing through the meteorological background. The upward orientation of the point cloud, though less distinct, indicates a decreasing impact of aerosols with increasing LTS. This may be linked to more frequently separated aerosol and cloud layers in high LTS environments, as Painemal *et al* (2014) have shown that the distance between aerosol and cloud layers is in part dependent on LTS in this region. In high aerosol environments, the weak and thus non-significant relationships no longer indicate ACI, log(AI) and log(CDR) are even positively associated in the BBS (r : 0.14 in BBS, −0.04

in OM). While the weak associations in the OM are likely due to the saturation of ACI, it seems plausible that the observed positive associations in the BBS are driven by meteorology, as large aerosol plumes from biomass burning may lie well above the cloud deck, not directly interacting with the clouds below. Absorbing aerosol plumes above the cloud deck may however induce a semi-direct effect by increasing LTS, subsequently reducing the entrainment rate at cloud-top. As Johnson *et al* (2004) state, this can increase moisture and cloud liquid water content.

Generally, the BBS is characterized by a more stable troposphere than the OM (mean LTS is 2.3 K higher in BBS). Comparing the point clouds in figures 2(b) and (c), a slight shift along the x axis can be noticed, as stable situations become more frequent with high aerosol loadings (≈5%). These two observations may be linked to the effect of strongly absorbing carbonaceous aerosol particles during the BBS on atmospheric stability (Wilcox 2010, Costantino and Bréon 2013), highlighting the interdependence of the considered processes. However, the relationship between aerosol loading and LTS may also be due to the seasonal cycle of LTS (Klein and Hartmann 1993) and atmospheric conditions that control the transport patterns of biomass burning aerosols to the Southeast Atlantic (Krishnamurti *et al* 1993, Garstang *et al* 1996).

Log(AI)–log(CDR) relationships are similarly sensitive towards large-scale RH (bottom row of figures). Relationships are mostly non-significant in situations with RH smaller than 60%. It is unlikely that clouds with such low grid RH represent a homogeneous stratocumulus cloud deck but rather thin or broken clouds. The observed weak relationships may thus be due to cloud field heterogeneity or to erroneous aerosol retrievals (Huang *et al* 2011, Grandey *et al* 2013). With RH > 60%, increases in RH tend to coincide with an increase in the strength of negative associations up to an RH of 80%, suggesting stronger ACI. In very humid conditions (RH > 90%) an increasing effect of RH on the relationship between log(AI) and log(CDR) is noticeable, leading to weaker associations in the case of a low-aerosol-loading environment and a distinct peak of positive associations in a high-aerosol-loading environment during the BBS. This apparent RH sensitivity may be due to the swelling of aerosols at high humidity levels and could thus be regarded as spurious in the context of ACI. However, as pointed out above, aerosols are thought to be frequently situated above the cloud deck in these situations. It is questionable to what extent large-scale information of boundary layer humidity is a good proxy for the humidity in the proximity of the aerosol particles.

As shown above, in addition to the seasonal component of ACI, there seem to be two distinct thermodynamic regimes controlling ACI intensity and thus cloud droplet size. Figure 3 proposes a conceptual framework summarizing possible and known mechanisms in the aerosol-stratocumulus-meteorology system in two contrasting thermodynamic environments (stable versus unstable). In each case, three pathways through which LTS, and in extension turbulent mixing, might affect cloud microphysics and ACI are illustrated:

(1) Cloud droplet growth dynamics (Matsui *et al* 2004). ACI susceptibility depends on droplet size (Platnick and Twomey 1994, Coakley and Walsh 2001).

(2) Mixing of aerosol and cloud layers, enabling ACI (Costantino and Bréon 2013, Painemal *et al* 2014).

(3) Dry air entrainment at cloud top and connected changes in RH (e.g. Johnson *et al* 2004, Kaufman *et al* 2005b, Tanré *et al* 2008).

In the proposed aerosol-stratocumulus-meteorology system, these mechanisms are controlled by the thermodynamic conditions (i.e. intensity of turbulent mixing). In an unstable environment, more turbulent mixing leads to increased mixing of aerosol and cloud layers (Painemal *et al* 2014), as well as increased ACI susceptibility due to larger cloud droplets (Platnick and Twomey 1994, Coakley and Walsh 2001), caused by dynamic droplet growth (Matsui *et al* 2004). These mechanisms increase ACI intensity, leading to the observed decrease in droplet size. Due to saturation, aerosols do not seem to have the same effect with high aerosol loading. Under these conditions, meteorology may be the main factor determining cloud microphysics. In the BBS, situations with high aerosol loading tend to feature larger droplets in the stable environment, possibly due to weaker dry air entrainment and water vapour that may be trapped beneath the inversion. These factors may lead to higher humidity levels, a higher LWP and thus larger droplets (Johnson *et al* 2004, Painemal *et al* 2014). This system would be in accordance with our findings, as aerosol impact on cloud microphysics seems to be practically confined to low aerosol loadings. When aerosol loading exceeds the point of saturation, meteorological factors, e.g. RH, gain importance. During the BBS, such situations with high humidity levels feature marked positive log(AI)–log(CDR) associations (figure 2(f)).

4. Conclusions

The aim of this study was to elucidate to what extent the magnitude of aerosol impact on cloud microphysics is controlled by the atmospheric aerosol loading and thermodynamics. Aerosol impact on cloud droplet size is highly variable as summarized in figure 3 and features a seasonal component due to the BBS. However, clear patterns for ACI can be identified under specific conditions: low-aerosol environments display pronounced negative associations between aerosols and cloud droplets and thus represent the

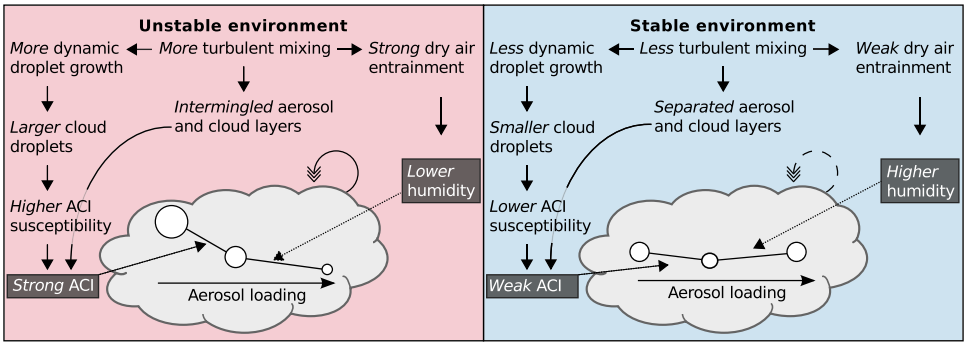

Figure 3. Influence of thermodynamic state on cloud droplet size and aerosol–cloud interactions (ACI) in environments with varying aerosol loadings.

scientific understanding of ACI. In these situations, the impact of thermodynamics and RH is noticeable; still, cloud microphysics seem to be dominated by aerosol effects. In low-aerosol environments, relationships are stronger in the BBS, possibly due to the high potential of the biomass burning particle species to act as CCN. In high-aerosol environments, aerosol impact on droplet size is hardly quantifiable, meteorological influences on cloud droplet sizes predominate, especially in the BBS, where the large aerosol plumes are thought to be well separated from the cloud deck.

The thermodynamic state seems to influence cloud droplet size and ACI. While there is good evidence for ACI in unstable environments, thermodynamically induced processes might impede ACI under stable conditions by various mechanisms. Additionally, the presented relationships may be indicative of aerosol swelling and cloud droplet growth in very humid conditions (starting at 80% RH, dominant with RH > 90%), possibly leading to the observed marked changes in aerosol–cloud droplet relationships, especially in the BBS. However, this finding needs further investigation as boundary layer humidity may not be representative of the humidity in the vicinity of the biomass burning aerosols. Based on these results, it may be possible to more fully understand the links between processes partaking in the aerosol-stratocumulus-meteorology system, ultimately reducing some of the uncertainties associated with ACI in this cloud regime.

Acknowledgments

MODIS data used in this study were acquired as part of the NASA's Earth–Sun System Division and archived and distributed by the MODIS Adaptive Processing System (MODAPS). MODIS data were obtained from the Goddard Space Flight Center (http://ladsweb.nascom.nasa.gov/data/search.html; accessed 21st October 2013). ECMWF ERA-Interim data used in this study were obtained from the ECMWF data server (http://apps.ecmwf.int/datasets/data/interim_full_daily/; accessed 7th October 2013). Funding for this study was provided by Deutsche Forschungsgemeinschaft (DFG) in the project GEOPAC (grant CE 163/5-1). The authors would like to thank J Fuchs for valuable discussions and comments on the manuscript. Constructive, insightful comments from two anonymous reviewers helped to greatly improve the manuscript.

References

Albrecht B A 1989 Aerosols, cloud microphysics and fractional cloudiness *Science* **245** 1227–30

Anderson B E, Grant W B, Gregory G L, Browell E V, Collins J E Jr, Sachse G W, Bagwell D R, Hudgins C H, Blake D R and Blake N J 1996 Aerosols from biomass burning over the tropical south atlantic region: distributions and impacts *J. Geophys. Res.* **101** 24117–37

Andreae M O and Rosenfeld D 2008 Aerosol cloud precipitation interactions. Part 1. The nature and sources of cloud-active aerosols *Earth-Sci. Rev.* **89** 13–41

Boucher O *et al* 2013 Clouds and aerosols *Climate Change 2013: The Physical Science Basis, Contribution of Working Group I to the Fourth Assessment Report of the Intergovernmental Panel on Climate Change* ed T F Stocker, D Qin, G K Plattner, M Tignor, S K Allen, J Boschung, A Nauels, Y Xia, V Bex and P M Midgely (Cambridge: Cambridge University Press)

Brenguier J-L, Pawlowska H, Schüller L, Preusker R, Fischer J and Fouquart Y 2000 Radiative properties of boundary layer clouds: droplet effective radius versus number concentration *J. Atmos. Sci.* **57** 803–21

Bréon F-M, Tanré D and Generoso S 2002 Aerosol effect on cloud droplet size monitored from satellite *Science* **295** 834–8

Charlson R J, Ackerman A S, Bender F M, Anderson T L and Liu Z 2007 On the climate forcing consequences of the albedo continuum between cloudy and clear air *Tellus* B **59** 715–27

Chen Y-C, Christensen M W, Stephens G L and Seinfeld J H 2014 Satellite-based estimate of global aerosol–cloud radiative forcing by marine warm clouds *Nat. Geosci.* **7** 643–6

Coakley J and Walsh C 2001 Limits to the aerosol indirect radiative effect derived from observations of ship tracks *J. Atmos. Sci.* **59** 668–80

Costantino L and Bréon F-M 2013 Aerosol indirect effect on warm clouds over South–East Atlantic, from co-located MODIS and CALIPSO observations *Atmos. Chem. Phys.* **13** 69–88

Dee D P *et al* 2011 The ERA-Interim reanalysis: configuration and performance of the data assimilation system *Q. J. R. Meteorol. Soc.* **137** 553–97

Edwards D P *et al* 2006 Satellite-observed pollution from southern hemisphere biomass burning *J. Geophys. Res.* **111** D14312

Garstang M, Tyson P D, Swap R, Edwards M, Kållberg P and Lindesay J A 1996 Horizontal and vertical transport of air over southern Africa *J. Geophys. Res.* **101** 23721

Grandey B S, Stier P and Wagner T M 2013 Investigating relationships between aerosol optical depth and cloud fraction using satellite, aerosol reanalysis and general circulation model data *Atmos. Chem. Phys.* **13** 3177–84

Hartmann D L, Ockert-Bell M E and Michelsen M L 1992 The effect of cloud type on earth's energy balance: global analysis *J. Clim.* **5** 1281–304

Haywood J M, Ramaswamy V and Donner L J 1997 A limited-area-model case study of the effects of sub-grid scale variations in relative humidity and cloud upon the direct radiative forcing of sulfate aerosol *Geophys. Res. Lett.* **24** 143–6

Huang J, Hsu N C, Tsay S-C, Jeong M-J, Holben B N, Berkoff T A and Welton E J 2011 Susceptibility of aerosol optical thickness retrievals to thin cirrus contamination during the BASE-ASIA campaign *J. Geophys. Res.* **116** D08214

Hubanks P A, King M D, Platnick S and Pincus R 2008 MODIS Atmosphere L3 Gridded Product Algorithm Theoretical Basis Document No. ATBD-MOD-30 for Level-3 Global Gridded Atmosphere Products (08_D3, 08_E3, 08_M3)

Johnson B T, Shine K P and Forster P M 2004 The semi-direct aerosol effect: impact of absorbing aerosols on marine stratocumulus *Q. J. R. Meteorol. Soc.* **130** 1407–22

Jones T A, Christopher S A and Quaas J 2009 A six year satellite-based assessment of the regional variations in aerosol indirect effects *Atmos. Chem. Phys.* **9** 4091–114

Kaufman Y J, Koren I, Remer L, Rosenfeld D and Rudich Y 2005a The effect of smoke, dust, and pollution aerosol on shallow cloud development over the Atlantic Ocean *Proc. Natl Acad. Sci. USA* **102** 11207–12

Kaufman Y J *et al* 2005b A critical examination of the residual cloud contamination and diurnal sampling effects on MODIS estimates of aerosol over ocean *IEEE Trans. Geosci. Remote Sens.* **43** 2886–97

Keil A and Haywood J M 2003 Solar radiative forcing by biomass burning aerosol particles during safari 2000: a case study based on measured aerosol and cloud properties *J. Geophys. Res. : Atmos.* **108** 8467

Klein S A and Hartmann D L 1993 The seasonal cycle of low stratiform clouds *J. Clim.* **6** 1587–606

Koshiro T and Shiotani M 2014 Relationship between low stratiform cloud amount and estimated inversion strength in the lower troposphere over the global ocean in terms of cloud types *J. Meteorol. Soc. Japan.* II **92** 107–20

Krishnamurti T N, Fuelberg H E, Sinha M C, Oosterhof D, Bensman E L and Kumar V B 1993 The meteorological environment of the tropospheric ozone maximum over the tropical South Atlantic Ocean *J. Geophys. Res.* **98** 10621

Labonne M, Bréon F-M and Chevallier F 2007 Injection height of biomass burning aerosols as seen from a spaceborne lidar *Geophys. Res. Lett.* **34** L11806

Levy R C, Remer L A, Tanré D, Mattoo S and Kaufman Y J 2009 Algorithm for remote sensing of tropospheric aerosol over dark targets from MODIS : collections 005 and 051 : Revision 2 ; Feb 2009 1–96

Loeb N G and Schuster G L 2008 An observational study of the relationship between cloud, aerosol and meteorology in broken low-level cloud conditions *J. Geophys. Res.* **113** D14214

Matsui T, Masunaga H, Kreidenweis S M, Pielke R A, Tao W-K, Chin M and Kaufman Y J 2006 Satellite-based assessment of marine low cloud variability associated with aerosol, atmospheric stability, and the diurnal cycle *J. Geophys. Res.* **111** D17204

Matsui T, Masunaga H and Pielke R A Sr 2004 Impact of aerosols and atmospheric thermodynamics on cloud properties within the climate system *Geophys. Res. Lett.* **31** L06109

Meyer K, Platnick S, Oreopoulos L and Lee D 2013 Estimating the direct radiative effect of absorbing aerosols overlying marine boundary layer clouds in the southeast Atlantic using MODIS and CALIOP *J. Geophys. Res.: Atmos.* **118** 4801–15

Myhre G, Stordal F, Johnsrud M, Kaufman Y J, Rosenfeld D, Storelvmo T, Kristjansson J E, Berntsen T K, Myhre A and Isaksen I S A 2007 Aerosol–cloud interaction inferred from MODIS satellite data and global aerosol models *Atmos. Chem. Phys.* **7** 3081–101

Nakajima T, Higurashi A, Kawamoto K and Penner J E 2001 A possible correlation between satellite-derived cloud and aerosol microphysical parameters *Geophys. Res. Lett.* **28** 1171–4

Painemal D, Kato S and Minnis P 2014 Boundary layer regulation in the southeast Atlantic cloud microphysics during the biomass burning season as seen by the A-train satellite constellation *J. Geophys. Res.: Atmos.* **119** 11288–302

Pincus R and Baker M B 1994 Effect of precipitation on the albedo susceptibility of clouds in the marine boundary layer *Nature* **372** 250–2

Platnick S, King M D, Ackerman S A, Menzel W P, Baum B A, Riédi J C and Frey R A 2003 The MODIS cloud products : algorithms and examples from terra *IEEE Trans. Geosci. Remote Sens.* **41** 459–73

Platnick S and Twomey S 1994 Determining the susceptibility of cloud Albedo to changes in droplet concentration with the advanced very high resolution radiometer *J. Appl. Meteorol.* **33** 334–47

Quaas J, Boucher O and Lohmann U 2006 Constraining the total aerosol indirect effect in the LMDZ and ECHAM4 GCMs using MODIS satellite data *Atmos. Chem. Phys.* **6** 947–55

Randall D A, Coakley J A Jr, Fairall C W, Kropfli R A and Lenschow D H 1984 Outlook for research on subtropical marine stratiform clouds *Bull. Am. Meteorol. Soc.* **65** 1290–301

Stevens B and Feingold G 2009 Untangling aerosol effects on clouds and precipitation in a buffered system *Nature* **461** 607–13

Stier P *et al* 2005 The aerosol-climate model ECHAM5-HAM *Atmos. Chem. Phys.* **5** 1125–56

Su W, Loeb N G, Xu K-M, Schuster G L and Eitzen Z A 2010 An estimate of aerosol indirect effect from satellite measurements with concurrent meteorological analysis *J. Geophys. Res.* **115** D18219

Tanré D, Artaxo P, Yuter S and Kaufman Y J 2008 *In situ* and remote sensing techniques for measuring aerosols, clouds and precipitation *Aerosol Pollution Impact on Precipitation : A Scientific Review* (Berlin: Springer) pp 188–263

Twomey S 1977 The influence of pollution on the shortwave Albedo of clouds *J. Atmos. Sci.* **34** 1149–52

Wilcox E M 2010 Stratocumulus cloud thickening beneath layers of absorbing smoke aerosol *Atmos. Chem. Phys.* **10** 11769–77

Wilson J, Cuvelier C and Raes F 2001 A modeling study of global mixed aerosol fields *J. Geophys. Res.* **106** 34081–108